JOURNAL OF SYNCHROTRON RADIATION
ISSN 1600-5775

Received 23 December 2014
Accepted 23 April 2015

Edited by A. Momose, Tohoku University, Japan

Keywords: synchrotron radiotherapy; energy spectra; treatment planning.

Energy spectra considerations for synchrotron radiotherapy trials on the ID17 bio-medical beamline at the European Synchrotron Radiation Facility

Jeffrey C. Crosbie,[a]* Pauline Fournier,[b] Stefan Bartzsch,[c,d] Mattia Donzelli,[e] Iwan Cornelius,[b,f] Andrew W. Stevenson,[f,g] Herwig Requardt[e] and Elke Bräuer-Krisch[e]

[a]School of Applied Sciences, RMIT University, Melbourne, Victoria, Australia, [b]Centre for Medical Radiation Physics, University of Wollongong, New South Wales, Australia, [c]Institute of Cancer Research, Sutton, Surrey, UK, [d]German Cancer Research Centre (DKFZ), Heidelberg, Germany, [e]European Synchrotron Radiation Facility, Grenoble, France, [f]The Australian Synchrotron, Clayton, Victoria, Australia, and [g]CSIRO, Clayton, Victoria, Australia.
*Correspondence e-mail: jeffrey.crosbie@rmit.edu.au

The aim of this study was to validate the kilovoltage X-ray energy spectrum on the ID17 beamline at the European Synchrotron Radiation Facility (ESRF). The purpose of such validation was to provide an accurate energy spectrum as the input to a computerized treatment planning system, which will be used in synchrotron microbeam radiotherapy trials at the ESRF. Calculated and measured energy spectra on ID17 have been reported previously but recent additions and safety modifications to the beamline for veterinary trials warranted a fresh investigation. The authors used an established methodology to compare X-ray attenuation measurements in copper sheets (referred to as half value layer measurements in the radiotherapy field) with the predictions of a theoretical model. A cylindrical ionization chamber in air was used to record the relative attenuation of the X-ray beam intensity by increasing thicknesses of high-purity copper sheets. The authors measured the half value layers in copper for two beamline configurations, which corresponded to differing spectral conditions. The authors obtained good agreement between the measured and predicted half value layers for the two beamline configurations. The measured first half value layer was 1.754 ± 0.035 mm Cu and 1.962 ± 0.039 mm Cu for the two spectral conditions, compared with theoretical predictions of 1.763 ± 0.039 mm Cu and 1.984 ± 0.044 mm Cu, respectively. The calculated mean energies for the two conditions were 105 keV and 110 keV and there was not a substantial difference in the calculated percentage depth dose curves in water between the different spectral conditions. The authors observed a difference between their calculated energy spectra and the spectra previously reported by other authors, particularly at energies greater than 100 keV. The validation of the beam spectrum by the copper half value layer measurements means the authors can provide an accurate spectrum as an input to a treatment planning system for the forthcoming veterinary trials of microbeam radiotherapy to spontaneous tumours in cats and dogs.

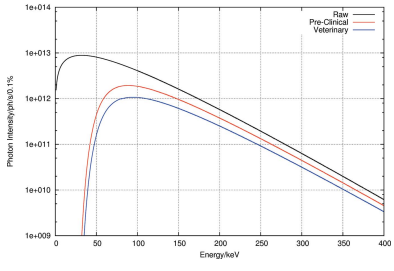

1. Introduction

Pre-clinical microbeam radiation therapy (MRT) studies have been performed on the ID17 beamline at the European Synchrotron Radiation Facility (ESRF) in Grenoble, France, for approximately ten years. For most of these studies, researchers have used tumour-inoculated rodents as the experimental subject (Bouchet *et al.*, 2010, 2013; Serduc *et al.*, 2009; Laissue *et al.*, 2007; Miura *et al.*, 2006). There has also been a significant amount of dosimetry work published

pertaining to MRT (Prezado *et al.*, 2011; Nettelbeck *et al.*, 2009; Siegbahn *et al.*, 2006; Brauer-Krisch *et al.*, 2003, 2005). The pre-clinical studies have shown very promising tumour control with minimal normal tissue complications. To this end, veterinary trials of cats and dogs bearing spontaneous tumours have now begun.

Radiation safety precautions for the veterinary clinical trials have necessitated the use of additonal ionization chambers and gas-filled flight pipes. The overall effect is to reduce the very high incident dose rate and to harden the X-ray beam relative to the pre-clinical energy spectrum condition. A computerized treatment planning system (TPS) for MRT trials using a fast analytical dose calculation algorithm is also under development (Bartzsch & Oelfke, 2013). The TPS requires the energy spectrum of the synchrotron-generated X-ray beam as an input. The energy spectrum of a kilovoltage X-ray beam has a direct influence on the dosimetric properties such as the depth of penetration of the beam and the range of scattered secondary electrons. Knowledge of the energy spectrum is important for both broad beam and microbeam radiotherapy studies. The aim of this current study is to provide an accurate energy spectrum as input to the MRT treatment planning system.

The energy spectrum of the pre-clinical beam on ID17 was previously measured using a powder diffraction technique and this spectrum was subsequently reported in other publications (Siegbahn *et al.*, 2006). Martínez-Rovira *et al.* recently reported calculated energy spectra for ID17 at different positions along the beamline (Martínez-Rovira *et al.*, 2012). They used a combination of the *SHADOW* ray-tracing code (Sanchez del Rio *et al.*, 2011) and the *PENELOPE* Monte Carlo package (Sempau *et al.*, 2011; Salvat *et al.*, 2009) in their paper. Given the various modifications to the beamline in preparation for the veterinary trials, it was considered prudent to verify the energy spectrum, but a complicated powder diffraction method was not possible owing to beam time and staffing constraints. In a recent publication, Crosbie *et al.* reported a straightforward method to validate a synchrotron X-ray beam spectrum by measuring the attenuation of X-ray intensity (air kerma rate) by copper sheets (the half value layer method) and comparing with a theoretical model (Crosbie *et al.*, 2013). The theoretical model uses the *SPECTRA* program (Tanaka & Kitamura, 2001) to simulate the energy spectrum for a given set of input parameters. The model also uses a MATLAB-based program called *Dose4IMBL*, originally developed for the Australian Synchrotron. The *Dose4IMBL* program takes the *SPECTRA*-generated spectrum and extracts a variety of theoretical dosimetric information such as half value layers and mean energy and allows quick comparisons between measured and theoretical data. In essence, this paper extends the work of Crosbie *et al.* (2013) by applying the established methodology to half value layer measurements taken on the ID17 beamline. We did not measure the ID17 energy spectrum but rather validated a calculated spectrum using attenuation measurements.

2. Materials and methods

The ESRF in Grenoble, France, is a third-generation electron synchrotron with an operating electron energy of 6 GeV and 43 active beamlines. The ESRF has been in general operation since 1994 and is Europe's brightest source of synchrotron X-rays. The maximum storage ring current is 200 mA and the circumference of the storage ring is 844 m.

2.1. The ID17 beamline

The ID17 beamline at the ESRF has been described in detail in several publications (Brauer-Krisch *et al.*, 2010; Nettelbeck *et al.*, 2009; Bravin, 2007); the 2012 and 2014 papers by Martínez-Rovira *et al.* and Cornelius *et al.* are perhaps the most comprehensive published descriptions of the beamline to date (Martínez-Rovira *et al.*, 2012; Cornelius *et al.*, 2014). Briefly, the source of the X-rays is a permanent-magnet wiggler, 1.5 m long, with a nominal magnetic field of about 1.6 T for a wiggler gap of 24.8 mm, used for the MRT studies. The synchrotron X-ray beam is transported *in vacuo* a distance of about 37 m from the source whereupon the beam enters an experimental hutch. The sample stage is located approximately 40 m from the source.

There are several *in vacuo* and *ex vacuo* absorbers in the beam path which serve to filter the energy spectrum. We consider two conditions: condition 1 corresponding to the pre-clinical conditions and condition 2 corresponding to the veterinary trial conditions, requiring the presence of additional items for safety reasons and decreasing the typical dose rate of approximately 70 Gy s^{-1} mA^{-1} to about 40 Gy s^{-1} mA^{-1}. For condition 1, the following *in vacuo* filters are in use: carbon (1.15 mm), aluminium (1.78 mm), beryllium (2.3 mm) and copper (1.04 mm). These filters harden the X-ray photon beam and remove low-energy photons (less than 30 keV). Condition 1 corresponds to the standard condition for pre-clinical MRT experiments in rodents and in fact has been the default configuration for several years. Condition 2 is used during the MRT veterinary trials and uses the same *in vacuo* filters as condition 1 plus the following additional filtration: a 2.2 m-long krypton gas pipe (maintained at an effective pressure of 85 mbar) (Requardt *et al.*, 2013), two redundant *in vacuo* Compton chambers (designed and built at the ERSF) comprising four aluminium electrodes (each one 0.5 mm thick) which are coated with gold (between 0.8 and 1.6 µm thick) (Berkvens *et al.*, 2013), and two redundant in-air monitoring ionization chambers (Bragg-peak ionization chambers; model 34070, PTW, Freiburg, Germany) with an equivalent PMMA thickness of 19 mm (PTW, personal communication). The Kr gas filter is designed to prevent an overexposure by absorbing the low-energy photons in the unlikely event of sudden failure (cracking) of the filters. The two redundant Compton chambers monitor the incident broad beam; their signals are cross-calibrated against the measured absolute dose. The two in-air Bragg peak ion chambers monitor the accumulated dose during the treatment, comparing the expected integrated dose every 500 µm of

vertical translation of the goniometer movement with the measured dose increment.

2.2. Energy spectra calculation

The raw and filtered energy spectra were calculated using the *SPECTRA* program (version 9.0) (Tanaka & Kitamura, 2001) and the *XOP* program (version 2.3) (Sanchez del Rio & Dejus, 2004). These two programs use an analytical approach to calculating the energy spectra. We used the most accurate estimates of the storage ring and radiation source (wiggler) parameters by consulting with the ESRF's machine control group. These parameters are shown in Fig. 1, a screenshot from the *SPECTRA* program. For the purposes of the calculation, we assumed the operating mode of the synchrotron was the so-called 7/8 + 1 filling mode; a train of 868 bunches (7/8 of the storage ring circumference) filled with 200 mA. The bunch length in millimetres is given by σ_z. The horizontal and vertical emittance of the electron beam in milliradians are given by ε_x and ε_y, respectively. The ID17 beamline is a low-β beamline and the values of the beta functions β_x and β_y and the dispersion functions η_x and η_y are shown in the screenshot. The inverse Lorentz factor for the electron beam is given by $1/\gamma$ and the electron beam dimensions, in micrometres, are given by σ_x and σ_y.

The permanent-magnet wiggler on ID17 has 10 × 15 cm periods with a total length of 1.5 m. The wiggler comprises 21 magnetic poles arranged as ten pairs of poles with an additional 11th pole which is not included in the calculation. The wiggler magnetic field B in the peak direction (B_y) is perhaps the most important variable when calculating energy spectra. The magnetic field determines the deflection parameter K. A double exponential model was used to interpolate previously measured wiggler-gap magnetic field values. The magnetic field at 24.8 mm wiggler gap was calculated to be 1.595 T. The *SPECTRA* and *XOP* programs allow the user to select the slit dimensions: X mm × Y mm, and a calculation point at an arbitrary distance from the source. We chose 10 mm × 0.5 mm at a distance of 40 m from the source. Both programs allow the user to calculate the effect of filters or absorbers on the beam energy spectrum. The user can enter elemental and material composition data (thickness, density) for the absorbers (filters) which attenuate the beam according to published tables from the National Institute of Standards and Technology (NIST).

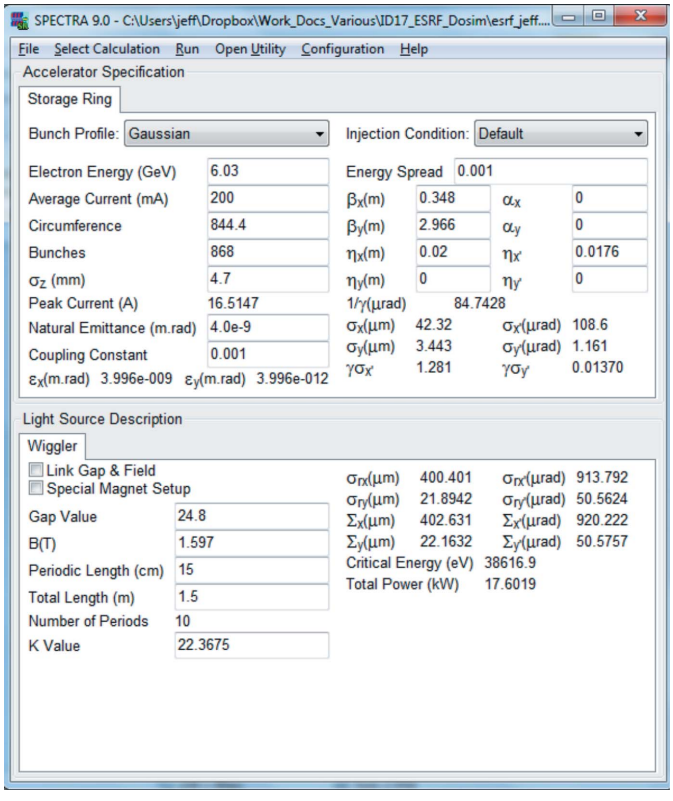

Figure 1
A screenshot from the *SPECTRA* program showing all parameters for the storage ring and wiggler radiation source for the ID17 beamline at the ESRF.

2.3. Experimental measurements

The principal technique employed in this study was the half value layer (HVL) method, using high-purity copper sheets. The HVL is defined as the thickness required to reduce the intensity (air kerma rate) of an X-ray beam to 50% of its original unattenuated value. The HVL technique is straightforward and routinely used in clinical radiotherapy dosimetry protocols in order to assess the energy of the X-ray beam in terms of millimetres of Cu (or Al). The penetrating properties of the beam were measured by conducting transmission measurements through copper sheets, and characterized by the first to third HVLs. We used high-purity copper (99.9% by weight) sheets measuring 100 mm × 100 mm with total thicknesses from 0.1 to 8.4 mm (Gammex 116 HVL attenuator set; Gammex Inc., Middleton, WI, USA). These sheets were placed normal to the beam. We used the PTW PinPoint ionization chamber (model No. 31014, PTW, Freiburg, Germany) to measure the transmitted signal. The PinPoint chamber is a small-volume cylindrical ionization chamber with an inner diameter of 2 mm and a sensitive volume of 0.015 cm^3. The ion chamber was connected to a PTW UNIDOS Webline Electrometer operating at a bias voltage of +400 V. The ion chamber (placed in air) was aligned parallel to the X-ray beam, which propagates horizontally into the experimental hutch. We used narrow-beam geometry conditions to just cover the ion chamber, thus ensuring the chamber only samples the primary fluence and not any extraneous scattered radiation (Khan, 2003). The horizontal and vertical beam dimensions were 10 mm × 0.5 mm and the chamber was moved vertically through the beam in order to simulate a uniform exposure to a quasi-10 mm × 10 mm field size. We did not observe any statistically significant ion chamber stem effects in this study. The HVL technique is a relative measurement, therefore conversion to absolute air kerma rate in Gy s^{-1} is not necessary, nor is correction for standard temperature and pressure a requirement. We took three readings for each copper thickness and averaged the reading. The readings were normalized to a storage ring current of

200 mA. We assigned a total uncertainty of ±2% to the ion chamber measurements, based largely on our previous experience (Crosbie *et al.*, 2013). The relative air kerma rate electrometer readings at each copper thickness (K_t) were normalized to the unattenuated zero copper thickness value (K_0). We took the negative logarithm of K_t/K_0, which is equal to a ray-sum, and plotted this ray sum as a function of absorber thickness. More formally, the log of the ratio of measured air kerma rate K_t to that for zero absorber thickness K_0 can be expressed as a function of the ray-sum,

$$-\ln\left(\frac{K_t}{K_0}\right) = \sum_L \mu t, \tag{1}$$

where the left-hand side is a function of two measured quantities, and the right-hand sum is the ray sum, equal to the sum of the product of attenuation coefficients and thickness for attenuating structures averaged across the beam area and along line L denoting the path of the ray. We can plot the ray sum (RS) as a function of thickness, describe the curve using a polynomial and solve for thickness x. An easier method uses the same functional model, but changes the variables around so that thickness is expressed as a function of the ray-sum,

$$x = a_0 + a_1\mathrm{RS} + a_2\mathrm{RS}^2. \tag{2}$$

In the present case, we work with the normalized air kerma rate K_t/K_0, so that $K_0 = 1.0$ and, since $\ln(K_0)$ is zero, then so is parameter a_0 (*i.e.* the curve passes through the origin). We use curve-fitting routines to find parameters a_1 and a_2, noting that higher-order coefficients are not required.

2.4. Comparison with theory

We used a MATLAB-based computer program called *Dose4IMBL* originally created for use on the Australian Synchrotron's Imaging and Medical Beamline. The mathematics behind *Dose4IMBL* are described by Crosbie *et al.* (2013) and will not be repeated here. *Dose4IMBL* reads in the *SPECTRA*-generated data file and extracts a variety of dosimetric information from the calculated energy spectra. *Dose4IMBL* is currently limited to only recognizing *SPECTRA*-generated files and not *XOP* data files; therefore all analysis of HVL and mean energy was done on the *SPECTRA*-generated data files. For a heterogeneous beam the first, second and third HVLs are defined as the thicknesses of filter material that reduces the air kerma rate K to 50%, 25% or 12.5% of its original value K_0, respectively. Having the air kerma expressed as a function of filter thickness made it a straightforward process to plot the function and extract the value for which $\ln(K/K_0) = \ln(0.5)$, $\ln(0.25)$ or $\ln(0.125)$ and compare the experimental HVLs with predicted HVLs. The relative uncertainty in predicted HVL is dominated by uncertainties in atomic cross sections, particularly at energies less than 30 keV. Gerward described uncertainties greater than 3% at 5–25 keV and 1–2% at higher energies (Gerward, 1993). We assigned a conservative uncertainty of 2% in μ_{en}, the mass energy absorption coefficient. We also assigned an uncertainty in the *in vacuo* filter thickness (0.5%) and filter orientation (0.8%). Since these error contributions are uncorrelated, they are combined in quadrature giving a total relative error for the theoretical HVL of ±2.2%. The mean energy of the beam was estimated assuming an energy-integrating detector. In simple terms, *Dose4IMBL* sums the product of energies and fluxes and divides by the fluxes to arrive at a mean energy [equation (15) of Crosbie *et al.* (2013)]. *Dose4IMBL* also calculates the predicted percentage depth dose in water by multiplying the theoretical air kerma rate by an exponential attenuation factor [equation (16) of Crosbie *et al.* (2013)].

3. Results

The calculated energy spectra for the wiggler-generated X-ray beam on the ID17 beamline are plotted in Fig. 2. The wiggler gap was 24.8 mm and the wiggler magnetic field was 1.595 T. Three spectra are plotted in Fig. 2: the raw (unfiltered) spectrum, the pre-clinical spectrum and the veterinary spectrum corresponding to the different configurations of beam filtering. The pre-clinical spectrum is dominated by 1.04 mm of *in vacuo* Cu, which removes soft X-rays below 30 keV. The veterinary spectrum includes two Bragg-peak ionization chambers which together were modelled as 19 mm of PMMA and had a marked effect on beam hardening and photon flux. The other absorbers in the path of the veterinary beam, *i.e.* the Kr gas pipe and the redundant Compton chambers (0.0016 mm Au and 2.0 mm Al), had very little effect on the spectra compared with the pre-clinical spectra (data not shown). The peak energies for the pre-clinical and veterinary configurations were 88 keV and 94 keV, respectively. The mean energies of the pre-clinical and veterinary configurations were 105 keV and 110 keV, respectively.

Fig. 3 shows a ray sum plot for the transmission of X-rays through the copper absorbers for the pre-clinical (Fig. 3*a*) and veterinary (Fig. 3*b*) X-ray beams. We obtained good agree-

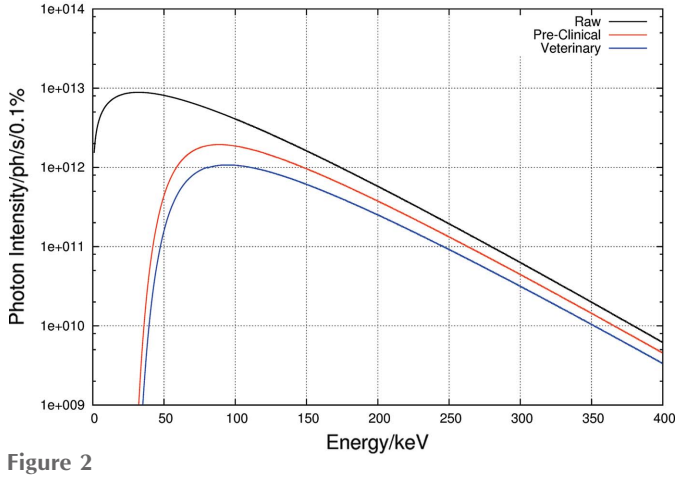

Figure 2
SPECTRA-calculated energy spectra for (*a*) the raw unfiltered X-ray beam from the ID17 wiggler, (*b*) the pre-clinical beam, dominated by 1.04 mm of Cu, and (*c*) the veterinary beam, which includes two Bragg-peak ionization chambers in the beam path, modelled as 19 mm of PMMA.

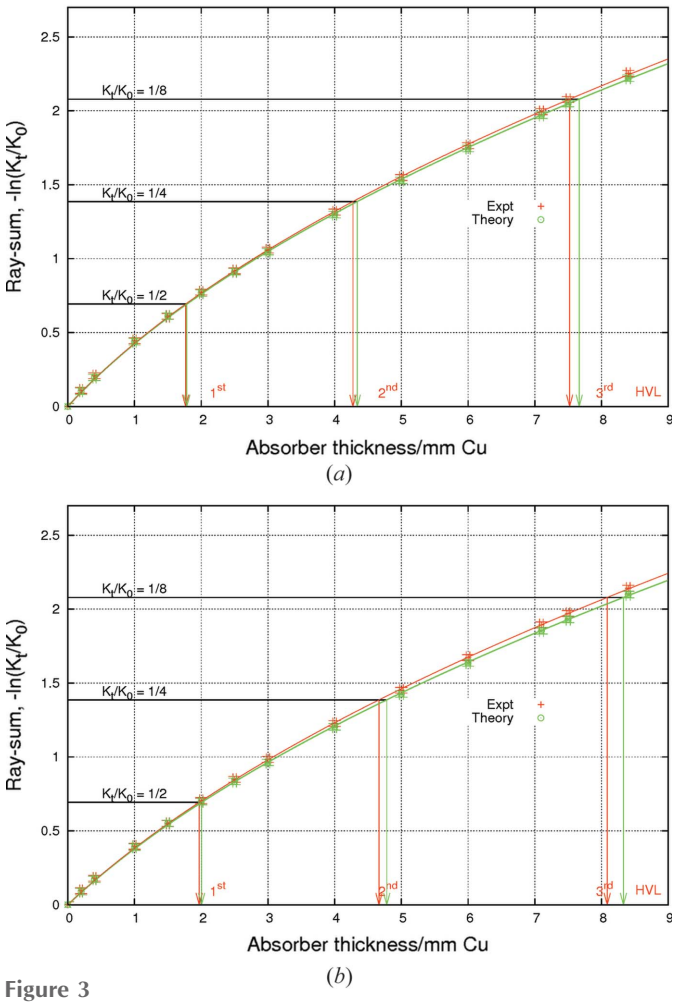

Figure 3
Ray-sum transmission curves for copper for the pre-clinical (*a*) and veterinary (*b*) spectral conditions showing good agreement between measured and theoretical values.

ment between measurement and theory for the pre-clinical spectra. Table 1 provides a summary of the measured and theoretical HVLs. The measured first HVL was 1.754 ± 0.035 mm Cu and 1.962 ± 0.039 mm Cu for the two spectral conditions, compared with theoretical predictions of 1.763 ± 0.039 mm Cu and 1.984 ± 0.044 mm Cu, respectively. The agreement between measurement and theory was not as good for the veterinary spectra but the deviation of the curves was within the limits of the error bars. The deviation was most marked for the third HVL.

We obtained excellent agreement between the *SPECTRA* and *XOP* codes as can be seen in the plots in Fig. 4 for the pre-clinical beams, normalized to their maximum values. We obtained moderate agreement between the *SPECTRA*/*XOP*-calculated energy spectra and the previously reported spectra: Fig. 2 of Siegbahn *et al.* (2006) and the vertical slit position from Fig. 3 of Martínez-Rovira *et al.* (2012). The deviations between the spectra were most pronounced at energies greater than 100 keV. There was also a systematic shift at lower energies (30–50 keV) between the *SPECTRA*/*XOP*-calculated energy spectra and the powder diffraction spectrum reported by Siegbahn *et al.*. There was less of a shift in energy

Table 1
Experimentally measured HVLs compared with theoretical predictions from the *Dose4IMBL* program for the pre-clinical and veterinary energy spectral conditions on ID17.

Pre-clinical	Experiment (mm Cu)	Theory (mm Cu)
HVL1	1.754 ± 0.035	1.763 ± 0.039
HVL2	2.550 ± 0.051	2.618 ± 0.057
HVL3	3.212 ± 0.064	3.278 ± 0.072

Veterinary	Experiment (mm Cu)	Theory (mm Cu)
HVL1	1.962 ± 0.039	1.984 ± 0.044
HVL2	2.747 ± 0.055	2.835 ± 0.063
HVL3	3.361 ± 0.067	3.476 ± 0.076

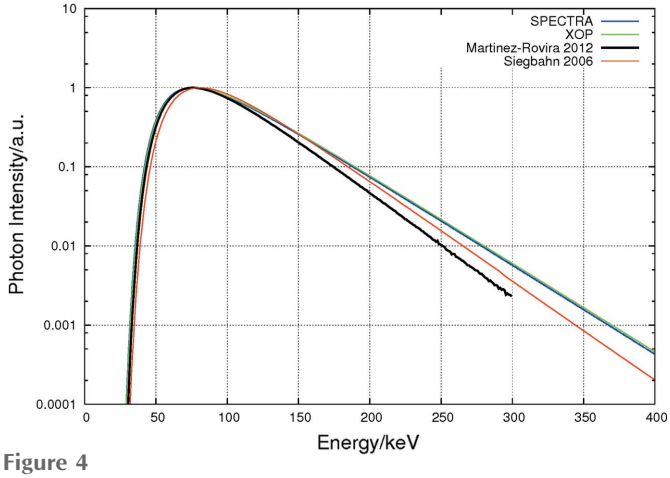

Figure 4
SPECTRA and *XOP*-calculated energy spectra for the pre-clinical X-ray beam on ID17 were in close agreement with one another. The energy spectra from Siegbahn *et al.* and Martinez-Rovira *et al.* were different from the current study, particularly at energies greater than 100 keV.

for the Martínez-Rovira *et al.* spectra, but poorer agreement at the higher energies. The *SPECTRA* and *XOP* codes produce a photon flux in units of photons s^{-1} (0.1% bandwidth)$^{-1}$. In other words the flux is reported in discrete bins of varying dimension as the energy increases (Tanaka & Kitamura, 2001; Sanchez del Rio & Dejus, 2004). We therefore divided the *SPECTRA* and *XOP*-produced photon flux by their energy in order to make a more meaningful comparison between the Siegbahn *et al.* and the Martinez-Rovira *et al.* energy spectra.

Fig. 5 shows a plot of the percentage depth dose (PDD) curve in water for the *SPECTRA*-calculated beam configurations. The PDD in water is an important dosimetric parameter, particularly when one is commissioning a treatment planning system. The two plots in Fig. 5 show that in fact there is not a large difference in PDD properties for the two beam configurations. The veterinary configuration was slightly more penetrating in water than the pre-clinical beam and these differences were most noticable in the 5–15 cm depth range.

4. Discussion and conclusions

We have shown in this paper our ability to validate a calculated energy spectrum on the ID17 beamline using a simple

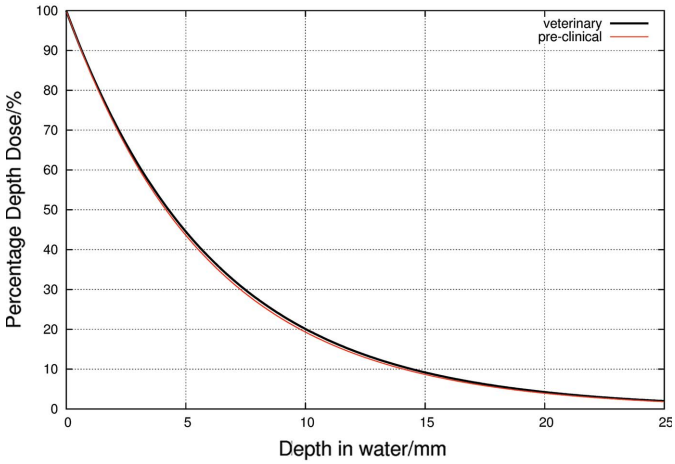

Figure 5
Predicted percentage depth dose (PDD) in water curves as calculated by the *Dose4IMBL* program using the pre-clinical and veterinary energy spectra from Fig. 2.

X-ray attenuation method. The HVL measurements in copper are easy to perform and closely agreed with our spectral calculations. We emphasize we have *not* measured the energy spectrum but rather used attenuation measurements to validate a calculated spectrum. The *Dose4IMBL* program proved to be a useful tool for quickly assessing the dosimetric effects of an altered beam spectrum; for example, the pre-clinical and veterinary configurations on ID17. The methodology reported here was recently described by Crosbie *et al.* (2013). The method relies heavily on knowing exactly what absorbers are in the path of the beam and the parameters of the storage ring and radiation source (*e.g.* wiggler). The ID17 beamline is a mature beamline at a 20 year old facility; therefore beamline components and storage ring parameters are well known and understood. The excellent agreement between measurement and theory for the pre-clinical configuration (Fig. 3*a*) is a testament to this fact. That we observed slightly poorer agreement for the new veterinary configuration (Fig. 3*b*) suggests slight deficiencies in how we modelled the material composition of the Bragg-peak ionization chambers and the Compton chambers. For example, the total thickness of the gold coating on the four aluminium electrodes was best estimated to between 0.8 and 1.6 µm; we used a 'worst-case' thickness in our calculations. There may also be an uncertainty on the density of Kr gas within the flight pipe.

The close agreement between the *SPECTRA* and *XOP* codes (Fig. 4) for the pre-clinical configuration was encouraging. In addition, we also obtained near-perfect agreement when we used an additional in-house energy spectra calculator code, independently developed by one of the co-authors (AWS, data not shown).

There is considerable room for future work using differing operating conditions, *e.g.* increased wiggler gaps to vary the energy spectrum and the flux rate. Another area which we have invested considerable efforts into is the topic of ionization chamber correction factors. The linear response of the ion chamber over the energy range is critical for absolute dosimetry, and in fact is the subject of a separate paper by the co-authors. Two separate correction factors are required here: a correction for ion recombination (k_s) and beam quality (k_Q). The co-authors have unpublished ion recombination data, obtained using a storage ring current ramping method; the only reliable way to reduce the dose rate without changing the energy spectrum. In summary, we observed a maximum value of k_s of 1.047 for the pre-clinical energy configuration. The beam quality correction factor, k_Q, for the PinPoint IC was stable over the energy range, based on calibration factors from the PTB primary standards laboratory in Germany (detailed data not shown). The PTB-supplied k_Q values were 0.950 (standard deviation 0.011) and 0.952 (standard deviation 0.015) for two separate PinPoint ion chambers across the energy range of interest on the ID17 beamline. The stability in k_Q in this energy range was reassuring to us. The details of our work in ion recombination and energy corrections for absolute dosimetry are the subject of a separate manuscript.

It is perhaps not too surprising that we did not obtain as good agreement between the *SPECTRA*/*XOP* data and the powder-diffraction measured spectrum from Siegbahn *et al.* and the Monte Carlo-calculated spectra of Martínez-Rovira *et al.*. These spectra from 2006 and 2012 were obtained *via* completely different methods and, in the case of Siegbahn *et al.*, the powder diffraction techique used to measure the ID17 energy spectra was performed over ten years ago using the methodology described by Honkimaki & Suortti (1992, 2007). It is possible that some beamline components (absorbing filters) and wiggler parameters (magnetic field) were not the same as the current setup. The shift in low energies for the 2006 spectrum indicates a difference in beam filtration; the 2006 spectrum was shifted towards higher energies compared with the other spectra, up to around 150 keV whereupon it overlaps and then diverges from the *SPECTRA*/*XOP* data. The 2012 spectrum more closely resembles our current data at low energies (less than 100 keV) but had poorer agreement at higher energies compared with the other spectra. Despite these differences, it was encouraging to note that the energy spectra were relatively similar to one another, considering the different ways they were recorded. Siegbahn *et al.* quoted the mean energy of the (pre-clinical) beam to be 107 keV in the interval 30–600 keV, whereas Martínez-Rovira *et al.* quoted the mean energy to be 99 keV in the same energy range. These authors further stated the peak energy was 75 keV and the final fraction of photons with energies higher than 300 keV was 0.1%. In our current study, we reported a mean energy (weighted average) of 105 keV for the pre-clinical configuration, in close agreement with the 2006 mean energy.

The PDD curves in Fig. 5 were quite insensitive to spectral changes compared with the ray-sum plots (Fig. 3). Whilst the PDD curves are undoubtedly useful from the perspective of the treatment planning system, they may not be the best way to compare different spectral configurations. The validation of the beam spectrum by the copper HVL measurements means we can provide an accurate spectrum as an input to a treatment planning system for the veterinary trials of MRT to spontaneous tumours in cats and dogs. We would advise other MRT developers around the world to ensure they provide a

validated energy spectrum to their planning system. We also recommend incorporating HVL measurements into a routine quality assurance program for any synchrotron radiotherapy trials. Accurate, absolute dose measurements are very important since any potential errors are propagated through the treatment planning system to the final dose prescription, while relative calculations such as the peak-to-valley dose ratio are rather robust to the small spectral changes. One could therefore use the same validated (veterinary) spectrum for any pre-clinical MRT studies.

Acknowledgements

The authors thank Dr Boaz Nash from the machine controls group at the ESRF for providing advice on storage ring parameters. JCC is an Early Career Research Fellow funded by the National Health and Medical Research Council (NH&MRC) of Australia. He was an employee of The University of Melbourne during his stay in France. JCC is grateful to Dr Alberto Bravin from the ESRF and Professor François Estève from INSERM U836 Equipe 6 for hosting his stay as a Visiting Scientist at the ESRF in 2012/2013. MD acknowledges financial support from the European Union's COST Action TD1205. PF and IC were funded by NH&MRC Development Grant 1017394. The authors thank Drs Immaculada Martínez-Rovira, Erik Siegbahn and Viejo Honkimäki for fruitful discussions relating to their work on energy spectra determination.

References

Bartzsch, S. & Oelfke, U. (2013). *Med. Phys.* **40**, 111714.
Berkvens, P., Brauer-Krisch, E., Brochard, T., Nemoz, C., Renier, M., Fournier, P., Requardt, H. & Kocsis, M. (2013). *Nuclear Science Symposium and Medical Imaging Conference (NSS/MIC)*, pp. 1–3. IEEE.
Bouchet, A., Lemasson, B., Christen, T., Potez, M., Rome, C., Coquery, N., Le Clec'h, C., Moisan, A., Bräuer-Krisch, E., Leduc, G., Rémy, C., Laissue, J. A., Barbier, E. L., Brun, E. & Serduc, R. (2013). *Radiother. Oncol.* **108**, 143–148.
Bouchet, A., Lemasson, B., Le Duc, G., Maisin, C., Bräuer-Krisch, E., Siegbahn, E., Renaud, L., Khalil, E., Rémy, C., Poillot, C., Bravin, A., Laissue, J., Barbier, E. & Serduc, R. (2010). *Int. J. Radiat. Oncol. Biol. Phys.* **78**, 1503–1512.
Bräuer-Krisch, E., Bravin, A., Lerch, M., Rosenfeld, A., Stepanek, J., Di Michiel, M. & Laissue, J. A. (2003). *Med. Phys.* **30**, 583–589.
Bräuer-Krisch, E., Requardt, H., Régnard, P., Corde, S., Siegbahn, E., LeDuc, G., Brochard, T., Blattmann, H., Laissue, J. & Bravin, A. (2005). *Phys. Med. Biol.* **50**, 3103–3111.
Brauer-Krisch, E., Serduc, R., Siegbahn, E. A., Le Duc, G., Prezado, Y., Bravin, A., Blattmann, H. & Laissue, J. A. (2010). *Mutat. Res.* **704**, 160–166.
Bravin, A. (2007). *The Biomedical Programs at the ID17 Beamline of the European Synchrotron Radiation Facility. Brilliant Light in Life and Material Sciences. NATO Security Through Science Series B; Physics and Biophysics.* The Netherlands: Springer.
Cornelius, I., Guatelli, S., Fournier, P., Crosbie, J. C., Sanchez del Rio, M., Bräuer-Krisch, E., Rosenfeld, A. & Lerch, M. (2014). *J. Synchrotron Rad.* **21**, 518–528.
Crosbie, J. C., Rogers, P. A. W., Stevenson, A. W., Hall, C. J., Lye, J. E., Nordström, T., Midgley, S. M. & Lewis, R. A. (2013). *Med. Phys.* **40**, 062103.
Gerward, L. (1993). *Radiat. Phys. Chem.* **41**,.
Honkimäki, V. & Suortti, P. (1992). *J. Appl. Cryst.* **25**, 97–104.
Honkimäki, V. & Suortti, P. (2007). *J. Synchrotron Rad.* **14**, 331–338.
Khan, F. M. (2003). *The Physics of Radiation Therapy*, 3rd ed. Philadelphia: Lippincott Williams and Wilkins.
Laissue, J., Blattmann, H., Wagner, H., Grotzer, M. & Slatkin, D. (2007). *Dev. Med. Child Neurol.* **49**, 577–581.
Martínez-Rovira, I., Sempau, J. & Prezado, Y. (2012). *Med. Phys.* **39**, 119–131.
Miura, M., Blattmann, H., Bräuer-Krisch, E., Bravin, A., Hanson, A. L., Nawrocky, M. M., Micca, P. L., Slatkin, D. N. & Laissue, J. A. (2006). *Br. J. Radiol.* **79**, 71–75.
Nettelbeck, H., Takacs, G. J., Lerch, M. L. & Rosenfeld, A. B. (2009). *Med. Phys.* **36**, 447–456.
Prezado, Y., Vautrin, M., Martínez-Rovira, I., Bravin, A., Estève, F., Elleaume, H., Berkvens, P. & Adam, J. (2011). *Med. Phys.* **38**, 1709–1717.
Requardt, H., Renier, M., Brochard, T., Bräuer-Krisch, E., Bravin, A. & Suortti, P. (2013). *J. Phys. Conf. Ser.* **425**, 022002.
Salvat, F., Fernandez-Verea, M. & Sempau, J. (2009). *PENELOPE 2008 – a code system for Monte Carlo simulation of photon and electron transport.* OECD Nuclear Energy Agency.
Sanchez del Rio, M., Canestrari, N., Jiang, F. & Cerrina, F. (2011). *J. Synchrotron Rad.* **18**, 708–716.
Sanchez del Rio, M. & Dejus, R. (2004). *Proc. SPIE*, **5536**,.
Sempau, J., Badal, A. & Brualla, L. (2011). *Med. Phys.* **38**, 5887–5895.
Serduc, R., Bouchet, A., Bräuer-Krisch, E., Laissue, J. A., Spiga, J., Sarun, S., Bravin, A., Fonta, C., Renaud, L., Boutonnat, J., Siegbahn, E. A., Estève, F. & Le Duc, G. (2009). *Phys. Med. Biol.* **54**, 6711–6724.
Siegbahn, E. A., Stepanek, J., Bräuer-Krisch, E. & Bravin, A. (2006). *Med. Phys.* **33**, 3248–3259.
Tanaka, T. & Kitamura, H. (2001). *J. Synchrotron Rad.* **8**, 1221–1228.